Solid State Communications 253 (2017) 31–36

Contents lists available at ScienceDirect

Solid State Communications

journal homepage: www.elsevier.com/locate/ssc

Communication

# Electronic and optical properties of $B_xN_yC_z$ monolayers with adsorption of hydrogen atoms

L. Leite[a], S. Azevedo[a,*], B. de Lima Bernardo[b]

[a] Departamento de Física, CCEN, Universidade Federal da Paraíba, Caixa Postal 5008, 58051-900 João Pessoa-PB, Brazil
[b] Departamento de Física, Universidade Federal de Campina Grande, 58429-140 Campina Grande-PB, Brazil

A B S T R A C T

We apply first-principles calculations, using density functional theory, to analyze the electronic and optical properties of monolayers of graphene with a nanodomain of 2D hexagonal boron nitrite (h-BN). It also investigated the effects of the adsorption of hydrogen atoms in different atoms at the edge of the h-BN nanodomain. We calculate the electronic band structure, the complex dielectric function and the optical conductivity. For such systems, the calculations demonstrate that the compounds exhibit a prominent excitement in the visible and near-infrared regions. In this form, the present study provides physical basis for potential applications of the considered materials in optoelectronic devices at the nanoscale.

## 1. Introduction

One of the main bases for the development of future technologies and other industries in the world today is the understanding of the fundamental properties of two-dimensional materials. Specifically, the studies of the electronic properties of graphene [1], its interactions with substrates [2], as well as the chemical doping process with other atoms aimed to tune its electronic properties [3] have been shown to provide many desired phenomena with the prospect for applications in technological devices.

Graphene is an allotropic form of carbon made by a monolayer of carbon atoms arranged in a honeycomb crystalline lattice with $sp^2$ hybridization, constituting the basic structural element of all other graphite materials. It can be experimentally obtained through the use of several methods, with the exfoliation of graphite as the easiest one. The most striking theoretical prediction, which was experimentally confirmed, is that electrons in graphene behave like massless Dirac fermions in a relativistic (1+2)-dimensional space–time [4]. Since its experimental discovery in 2004, [5], this material has drawn considerable attention of the scientific community. Particularly, it does not exhibit a band gap around the Fermi level, which, in principle, turns out to be unviable for the fabrication of electronic devices. However, there exist several methods for opening the graphene band gap, of which one of the most practical is by doping the structure with boron and nitrogen atoms [6].

The combination of the graphene monolayer with boron nitride nanodomains, such as $B_xN_yC_z$, has been shown to be an efficient method to engineer bandgaps in graphene, giving rise to a number of physical properties and a variety of possible technological applications [7]. Unfortunately, such compounds are not easy to synthesize when compared, for example, to carbon and boron nitride structures. However, from 2010, atomic layers of (hybrid) h-BNC materials, consisting of domains of BN and graphene, have been synthesized [8]. In that contribution, it was reported the obtention of h-BNC materials, consisting of hybridized, randomly distributed domains of h-BN and C phases with compositions ranging from pure BN to graphene. It was shown that the edge atoms of the $B_xN_yC_z$ nanodomain behave like acceptor states that are introduced by the substitutional boron atoms that form the C–B bonds at the nanodomain boundaries (see also Ref. [9]). On the other hand, donor states can be also introduced by the C–N bonds at the edge of the domains. In this form, it is possible to try to control the gap energy associated to impurities by varying the number of C–B and C–N bonds at the domain boundary. Such processes also give rise to energy states in the gap region. As a matter of fact, the impurity gap can be tuned by varying the domain size [10]. Therefore, due to this important characteristic, it has appeared a number of experimental growth attempts of such 2D hybrid materials [11–14].

It is also remarkable that graphene has been recognized as a revolutionary material for optoelectronic purposes. Indeed, we have witnessed recently many promising applications of graphene in various devices, such as transparent electrodes, ultrafast lasers, polarizers and photodetectors [15–18]. The low absolute value of light absorption of graphene (2.3% of the incident light is absorbed in the visible region)

* Corresponding author.
*E-mail addresses:* lazaroleite@hotmail.com.br (L. Leite), sazevedo@fisica.ufpb.br (S. Azevedo), bertulio.fisica@gmail.com (B. de Lima Bernardo).

http://dx.doi.org/10.1016/j.ssc.2017.01.025
Received 9 July 2016; Received in revised form 30 December 2016; Accepted 27 January 2017
Available online 28 January 2017
0038-1098/

limits the photocurrent efficiencies of graphene-based photodetectors [19,20]. Therefore, one of the main challenges is to enhance its optical absorption.

In this work, it is proposed a scenario in which the nanostructure of graphene with a boron nitrite (h-BN) nanodomain, as well as with the adsorption of hydrogen atoms at the edge of the h-BN nanodomain, allows an increased light absorption in the visible spectrum, which is in principle tunable. We present a theoretical study about the electronic and optical properties of a $B_xN_yC_z$ monolayer with the adsorption of hydrogen atoms. First, we show that the adsorption of hydrogen atoms is more stable at the edge of the h-BN nanodomain. Second, we evaluate the electronic properties by means of the analysis of the band structure, from which both the gap and the magnetic moment are calculated. Finally, we provide the optical properties of the compounds, namely, the real and imaginary parts of the dielectric function, which are related to the refractive index and absorption coefficient, respectively. Our results show that the studied materials have an enhanced optical absorption in the visible range as well as an enhanced electrical conductivity when compared to graphene.

## 2. Computational Methodology

All calculations were performed using the SIESTA program (Spanish Initiative for Electronic Simulations with Thousand of Atoms) [21], which makes use of the density-functional theory (DFT) [22]. The chosen functional exchange and correlation was the approximation Generalized Gradient Functional (GGA) in the form of the Perdew–Burke–Ernzerhof (PBE) correction [23]. The interaction between cores and valance electrons are presented by the Troullier–Martins norm-conserving pseudopotential [24]. A linear combination of numeric atomic orbitals is used to represent a double-$\zeta$ basis set with polarized functions (DZP). All the geometries are fully relaxed, with residual forces smaller than 0.1 eV/Å. Here, the total number of atoms included in the supercells is 160, and the unitary cell is repeated in the $X$ and $Y$ directions. A vacuum distance of 20/Å along the $Z$-axis was used to avoid interactions. The cut-off energy determining the density of the utilized real space grid has been set to 150 Ry, and the Brillouin zone was sampled with 4×4×2 $k$-points within the Monkhorst–Pack scheme.

All the structures of the materials to be explored herein are shown in Fig. 1. In Fig. 1a we have a graphene monolayer; Fig. 1b shows a monolayer of boron nitrite (h-BN); in Fig. 1c we see the monolayers of graphene with a $B_{27}N_{27}$ (27 atoms of boron and 27 atoms of nitrogen) nanodomain; Fig. 1d shows the $N_{27}B_{27}$–$H^{I}$ structure, where a hydrogen atom is adsorbed on the top of the supercell by a carbon atom which is bonded to boron; in Fig. 1e we have the $N_{27}B_{27-1}H^{I}$ arrangement, in which two hydrogen atoms are adsorbed on a carbon atom which is bonded to boron, where the H represents the hydrogen atom adsorbed on the bottom of the supercell; Fig. 1f exhibits the $B_{27}N_{27-1}HH^{I}$ structure, where we have a hydrogen atom adsorbed by a carbon atom which is bonded to the nitrogen atom on the bottom of the supercell and another adsorbed by a carbon atom which is bonded to the boron atom on the top of the supercell; Fig. 1g shows the $B_{27}N_{27}$–$H^{I}$ configuration, where a hydrogen atom is adsorbed on the top of supercell by a carbon atom which is bonded to nitrogen. Finally, in Fig. 1h we show the $B_{27}N_{27-1}H^{I}$ configuration, characterized by two hydrogen atoms adsorbed by the carbon atom which is bonded to the nitrogen atom.

The optical properties were calculated by using the frequency dependent complex dielectric function: $\epsilon(\omega) = \epsilon_1(\omega) + i\epsilon_2(\omega)$. The imaginary part is directly proportional to the optical absorption spectrum, which is calculated by means of a time dependent perturbation theory in the simple dipole approximation that is given by

$$\mathrm{Im}[\epsilon(\omega)] = \epsilon_2(\omega) = \frac{8\pi^2 e^2}{m^2\omega^2\Omega}\sum_{cv}\sum_{\mathbf{k}}|\langle\psi_{c\mathbf{k}}|\hat{\mathbf{e}}\cdot\mathbf{p}|\psi_{v\mathbf{k}}\rangle|^2 \times \delta(E_{c\mathbf{k}} - E_{v\mathbf{k}} - \hbar\omega), \tag{1}$$

for a vertical transition from a filled valence band $|\psi_{v\mathbf{k}}\rangle$ of energy $E_{v\mathbf{k}}$ to an empty conduction band $\langle\psi_{c\mathbf{k}}|$ of energy $E_{c\mathbf{k}}$ with the same wave vector $\mathbf{k}$ [25]. The parameter $\omega$ is the frequency of the incident radiation in energy units, $\Omega$ represents the volume of the supercell, $m$ is the electron mass, $\mathbf{p}$ is the momentum operator, and $\hat{\mathbf{e}}$ is the unit vector of polarization in the direction of the incident electric field. The real part of $\epsilon(\omega)$ is not independent of the imaginary part; they are related to each other by the Kramers–Kronig relation [26]. All the other optical constants can be derived from $\epsilon_1(\omega)$ and $\epsilon_2(\omega)$ such as the electrical conductivity which is given by

$$\sigma(\omega) = \mathrm{Re}\left[-i\frac{\omega}{4\pi}(\epsilon - 1)\right], \tag{2}$$

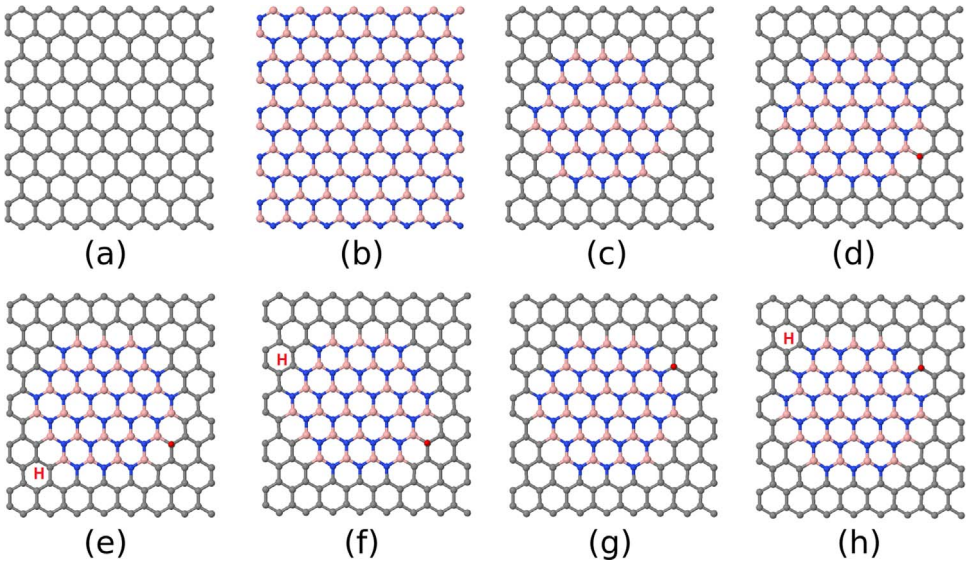


**Fig. 1.** (Color online) All analyzed configurations. The geometry of the supercell used in the calculations can be seen in (a) graphene, (b) boron nitrite (h-BN), (c) graphene with a $B_{27}N_{27}$ nanodomain, (d) $N_{27}B_{27}$–$H^{I}$ structure, in which one hydrogen atom is adsorbed on the top of the supercell, (e) $N_{27}B_{27-1}H^{I}$ structure, in which two hydrogen atoms are adsorbed; the character H in red represents the hydrogen on the bottom of the supercell, (f) $B_{27}N_{27-1}HH^{I}$ structure, in which two hydrogen atoms are adsorbed by the carbon bonded to different atoms, (g) $B_{27}N_{27}$–$H^{I}$ structure, in which one hydrogen atom is adsorbed by the carbon bonded to nitrogen, (h) $B_{27}N_{27-1}H^{I}$ structure, in which two hydrogen atoms are adsorbed by the carbon atom bonded to nitrogen.

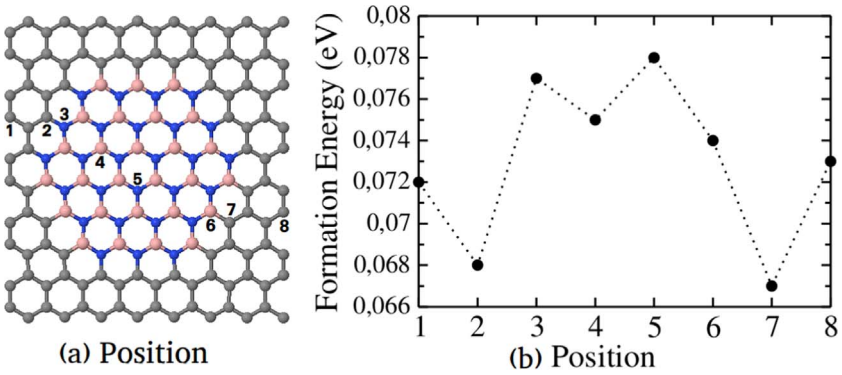


**Fig. 2.** Adsorption energy of a single hydrogen atom with respect to its position in the monolayer. In (a) we have a schematic description of the supercell. Numbers in black marked in the sites denote the different adsorption positions. (b) Formation energy of a hydrogen atom as a function of the positions. The dotted line is a visual guide.

where Re denotes the real part.

## 3. Results and discussion

### 3.1. Stability

To start with, we analyze the stability of the monolayer of graphene with a $B_{27}N_{27}$ nanodomain with respect to the different positions of adsorption of hydrogen atoms. The formation energy is calculated by simulating the chemical environment where the structure is synthesized [27]. In this case, the formation energy can be written as

$$E_{for} = (E_{tot} - n_B\mu_B - n_N\mu_N - n_C\mu_C - n_{HB}\mu_{HB} - n_{HN}\mu_{HN} - n_{HC}\mu_{HC})/n_{atoms}, \quad (3)$$

where $E_{tot}$ is the total energy calculated by SIESTA, $n_B$, $n_N$, $n_C$ are the numbers of atoms of B, N and C, respectively. $n_{HB}$, $n_{HN}$ and $n_{HC}$ are the numbers of B–H, N–H, and C–H bonds, respectively. $\mu_B$, $\mu_N$, $\mu_C$, $\mu_{HB}$, $\mu_{HN}$ and $\mu_{HC}$ represent the respective theoretical chemical potentials [28], and $n_{atoms}$ is the total number of atoms.

In Fig. 2, we can see that it is more energetically favorable for a single hydrogen atom to be adsorbed on a carbon atom attached to the boron or the nitrogen atom. The present result is consistent with the first-principles calculations that studied the adsorption energy of atomic hydrogen on a graphene surface and on the boron nitride/graphene monolayer interface [29,30].

### 3.2. Electronic properties

To better understand the adsorption of hydrogen atoms H on the monolayers of graphene with a h-BN domain, we calculate the band structure of all configurations shown in Fig. 1. Firstly, we focus on the structures without adsorption. The band structure of these systems can be seen in Fig. 3.

The band structure of the configurations shown in Fig. 3a (graphene), Fig. 3b, boron nitrite (h-BN), and in Fig. 3c (graphene with a $B_{27}N_{27}$ nanodomain) shows that these systems are semi-metallic, insulator and semiconductor, respectively. The structure shown in Fig. 3c has the same number of electrons of their parental compounds, i.e., it is isoelectric, and, for this reason, there are no extra charge carriers. Thus, there are no midgap states. It is important to notice that all structures without hydrogen adsorption have no magnetic moment. This happens because there is no imbalance in the $\pi$–$\pi^*$ system, since there is no disappearance of $p_z$ orbitals.

Now let us analyze the electronic properties of the structures on which the H atoms are adsorbed by the carbon atom which is bonded to boron in the same sublattice. The band structure of such systems is shown in Fig. 3d, for the adsorption of a single hydrogen atom, and in Fig. 3e, for the adsorption of two hydrogen atoms. The structures are semiconductors and have a non-zero magnetic moment. In these structures, we can see that two midgap polarized spin states are generated for each hydrogen atom adsorbed, and, due to the exchange-correlation, they are not degenerated. This is a well known and expected behavior, which is caused by the disappearance of the carbon $p_z$ orbital due to the rehybridization from $sp^2$ to $sp^3$ [31]. It was shown in Ref. [32] that a band gap of 1.25 eV is opened upon hydrogen adsorption in pristine graphene. Furthermore, it was demonstrated that this band gap is caused by the $H^+$ ion.

Fig. 3f shows the band structure of the configuration in which two hydrogen atoms are adsorbed by the carbon attached to different atoms. These configurations have no net spin because when the hydrogen atom is attached to the carbon atom which is bound to either a boron or a nitrogen atom, we have the formation of a electron–hole pair. Besides, we can see that the midgap states generated by the adsorbed H atoms are a consequence of the breaking of the double carbon bonds.

On the other hand, when we analyze the systems in which the H atoms are adsorbed on the carbon atom which is bound to nitrogen in the same sublattice, as shown in Figs. 3g and h, it is possible to verify that all structures are semiconductors, which is a usual behavior for hydrogen adsorption in hybrid monolayers, as well as the appearance of net spin due to the presence of the hydrogen atom.

### 3.3. Optical properties

In this section we investigate the optical properties of the compounds analyzed above. In Figs. 4–6 we show both the real and imaginary parts of the dielectric permittivity, as well as the conductivity of the aforementioned materials in comparison with those of the graphene and BN structures. Specifically, in Figs. 4(d), 5(d) and 6(d) we observe the behavior of the imaginary part of the permittivity, which is related to the light absorption properties of the structures. As we can see, for graphene we have a continuous energy range of absorption, which is characteristic of a semimetal, with two well defined peaks representing the regions in which the density of states is bigger, and a low absorption region around 2 eV corresponding to the Dirac point region. On the other hand, for the BN monolayer, we observe absorption only for energy values larger than 4.5 eV, which characterizes an insulator.

The situation is more interesting when hydrogen atoms are adsorbed at the edge of the BN domain in the graphene monolayer as, for example, in the $B_{27}N_{27}$–$H^1$ and $B_{27}N_{27-1}H^1$ monolayers, also shown in Figs. 4 and 5. In such cases we observe the appearance of a family of absorption peaks from 0.5eV to 2.5 eV, followed by a continuous region of absorption for larger energy values. Such absorption peaks represent an (excitonic) signature of the $e$–$h$ pairs naturally formed in these structures due to the C–B and C–N bonds. Indeed, the energy gap variations in hybrid structures take place from the electrons and holes created by the C–B and C–N bonds at the domain boundary.

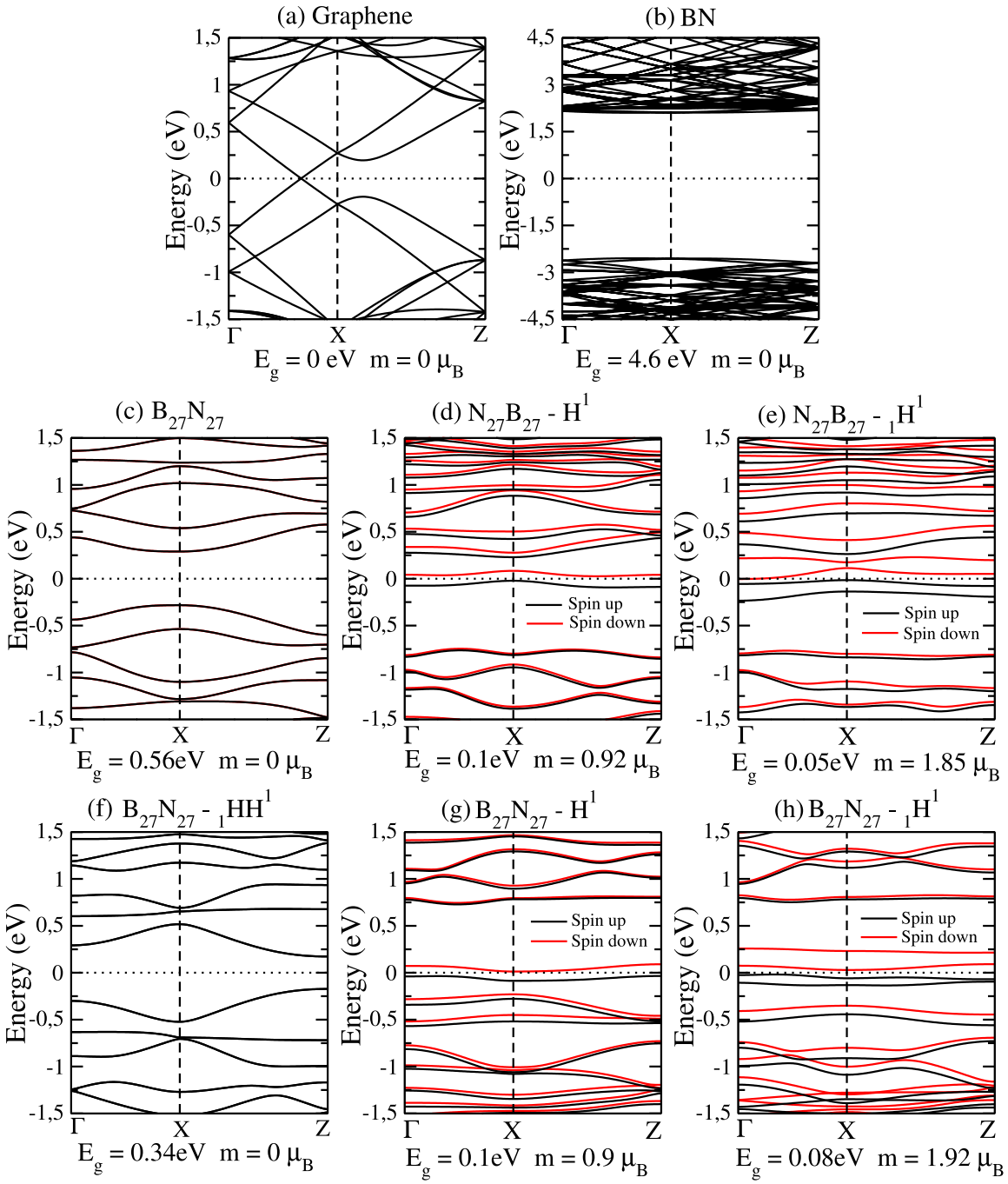


**Fig. 3.** (Color online) Calculated band structures of the studied configurations. The energy is scaled with respect to the Fermi energy (dotted line). $E_g$ is the energy of the band gap, $m$ is the magnetic moment and $\mu_B$ denotes the Bohr magneton. Spin-up and spin-down channels are represented by black and red lines, respectively.

Not less important, it can also be seen from Figs. 4 to 6 that the hybrid structures absorb more light in comparison with graphene in all the studied energy ranges. In this sense, the location and number of hydrogen atoms adsorbed at the boundary domain serve as an adjustment method for tuning the intensity and frequency of the absorbed light. These two last aspects can make the hydrogenated hybrid structures studied here important candidates for future optoelectronic implementations at the nanoscale, similar to those shown in Ref. [10].

Further calculations of the absorptive properties have shown that the hybrid structures absorb on average 48% of the light ranging from the near infrared to the near ultraviolet spectrum (1.2–5.1 eV). This is considerably more than the graphene monolayer, which absorbs roughly 15% in the same range, and the BN monolayer which absorbs around 4% of the light in the referred spectrum, most of it in the near ultraviolet region. Such property of hybrid monolayers raises the possibility of applications in solar energy conversion systems. About the electrical conductivity properties, it is shown in Figs. 4–6 the behavior of the hybrid structures in comparison with the graphene and BN monolayers. In all the cases, we can see that the hybrid materials conduct considerably more than graphene, with the exception of the $B_{27}N_{27}$ structure that presented a small energy gap of approximately 0.5 eV, which is a characteristic of a semiconductor. The other hybrid materials can be classified as metallic [33]. In this sense, the presence of the adsorbed hydrogen atom is decisive for the transition from the semiconducting to the metallic behavior. This is probably a conse-

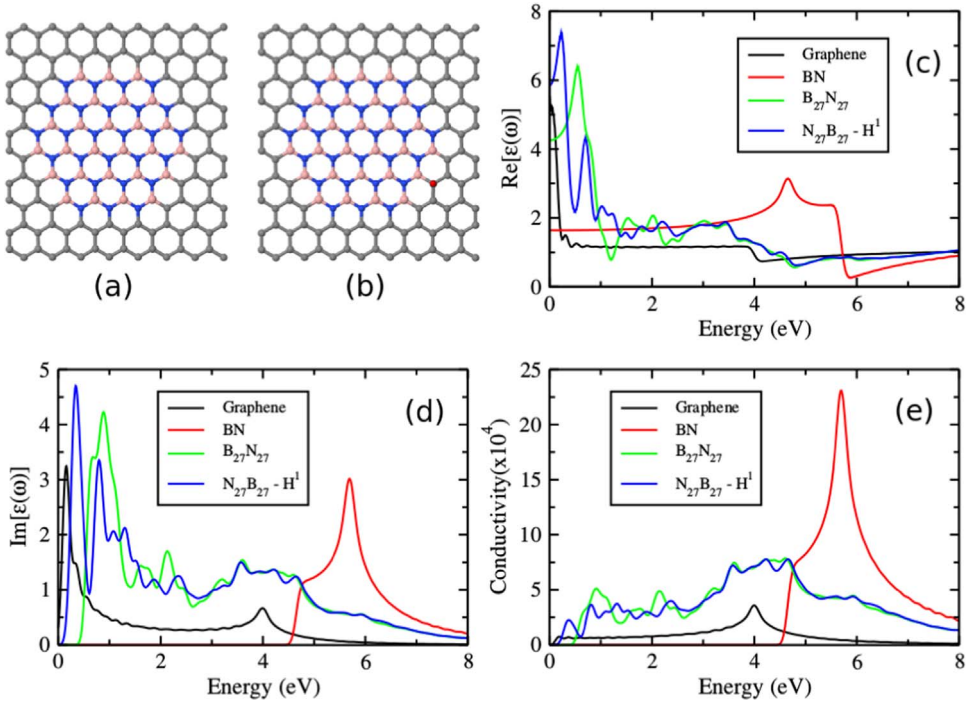


**Fig. 4.** Representation of the (a) graphene monolayers with a $B_{27}N_{27}$ and a (b) $N_{27}B_{27}$–$H^1$ domain. In (c) and (d) we have, respectively, the profiles of the real and imaginary parts of the electric permittivity as a function of the excitation energy, in comparison with those for the graphene and BN monolayers. The conductivity properties are shown in (e).

quence of the electron–hole pairs formed due to the adsorption of hydrogen.

## 4. Conclusions

In conclusion, we investigated the electronic structure and light absorption properties of graphene monolayers with boron nitrite nanodomains in the presence of hydrogen atoms adsorbed at the boundary of the domain. We used density functional theory to realize the calculations, which provided evidences about the enhanced absorptive properties of such materials, when compared to graphene, as well as the formation of exciton-like absorption peaks at the near infrared region. Interestingly, it was observed that the absorption spectrum of the studied hybrid structures presented a fine dependence on the location and number of adsorbed hydrogen atoms. In this regard, the present work introduces the idea that the usage of graphene monolayers with boron nitrite domains and the deposition of hydrogen atoms can be useful for optoelectronic purposes at the nanoscale, once

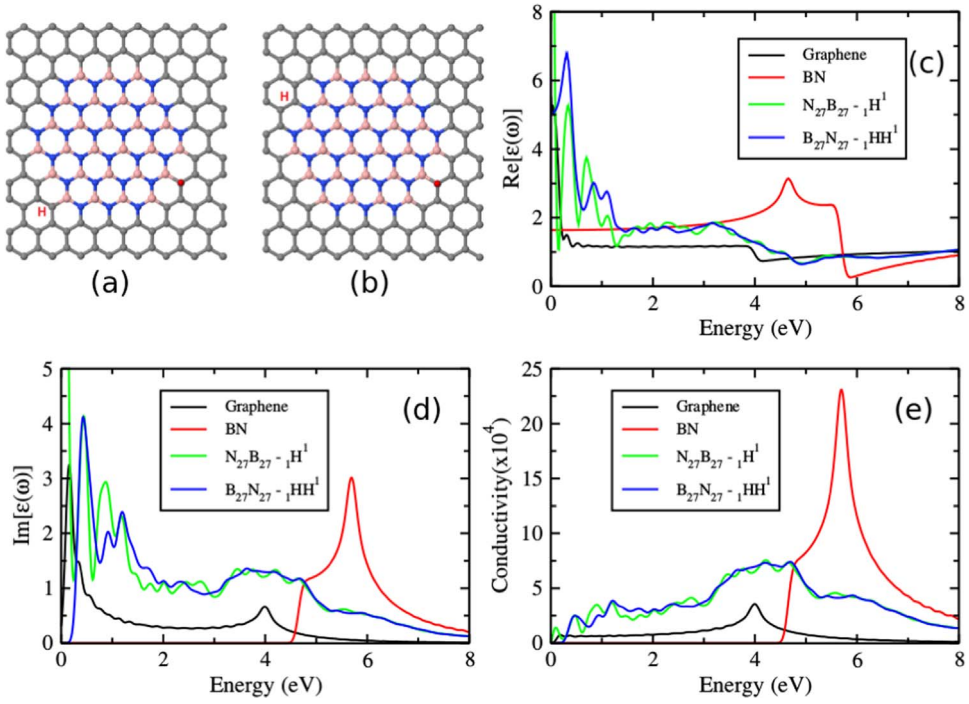


**Fig. 5.** Representation of the (a) graphene monolayers with a $N_{27}B_{27}$–$_1H^1$ and (b) $B_{27}N_{27}$–$_1HH^1$ domain. In (c) and (d) we have, respectively, the profiles of the real and imaginary parts of the electric permittivity as a function of the excitation energy, in comparison with those for the graphene and BN monolayers. The conductivity properties are shown in (e).

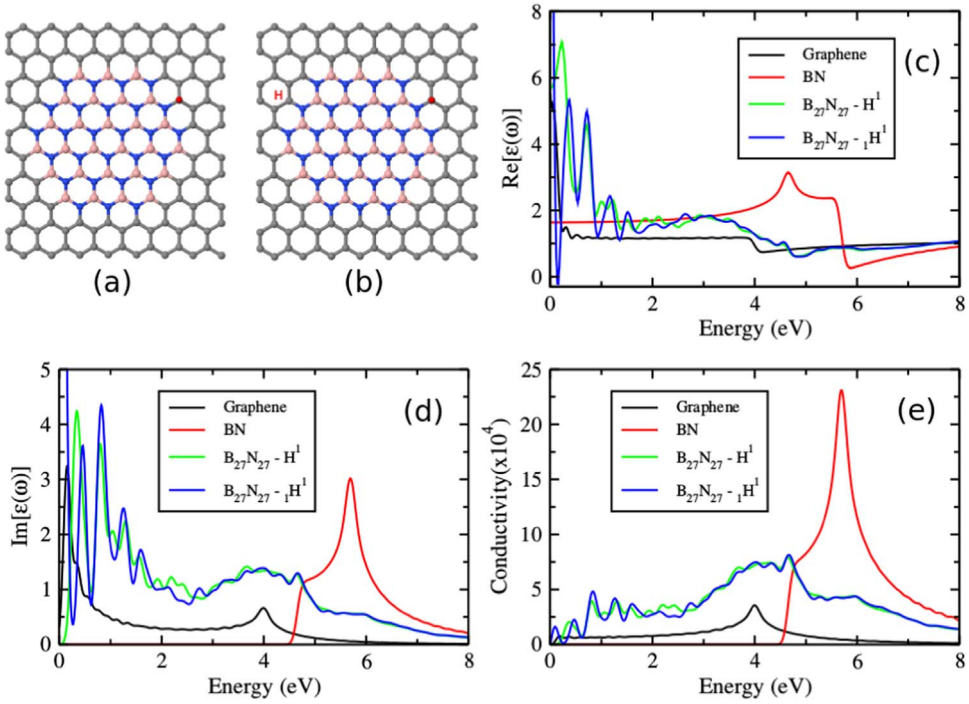


**Fig. 6.** Representation of the (a) graphene monolayers with a $B_{27}N_{27}$–$H^1$ and (b) $B_{27}N_{27}$–$_1H^1$ domain. In (c) and (d) we have, respectively, the profiles of the real and imaginary parts of the electric permittivity as a function of the excitation energy, in comparison with those for the graphene and BN monolayers. The conductivity properties are shown in (e).

such nanomaterials are absorptive and present a fine adjustment with respect to both the frequency and intensity of the absorbed light.

## Acknowledgments

We would like to thank to the INCT – Nanomateriais de Carbono and CNPq.

## References

[1] A.H. Castro Neto, F. Guinea, N.M.R. Peres, K.S. Novoselov, A.K. Geim, Rev. Mod. Phys. 81 (2009) 109.
[2] A.K. Geim, K.S. Novoselov, Nat. Mater. 6 (2007) 183.
[3] S.S. Yamijala, A. Bandyopadhyay, S.K. Pati, J. Phys. Chem. C 117 (2013) 23295.
[4] K.S. Novoselov, A.K. Geim, S.V. Morozov, D. Jiang, M.I. Katsnelson, I.V. Grigorieva, S.V. Dubonos, A.A. Firsov, Nature 438 (2005) 197.
[5] K.S. Novoselov, A.K. Geim, S.V. Morozov, D. Jiang, Y. Zhang, S.V. Dubonos, I.V. Grigorieva, A.A. Firsov, Science 306 (2004) 666.
[6] L.S. Panchakarla, K.S. Subrahmanyam, S.K. Saha, A. Govindaraj, H.R. Krishnamurthy, U.V. Waghmare, C.N.R. Rao, Adv. Mater. 21 (2009) 4726.
[7] A. Rubio, Nat. Mater. 9 (2010) 379.
[8] L. Ci, L. Song, C. Jin, D. Jariwala, D. Wu, Y. Li, A. Srivastava, Z.F. Wang, K. Storr, L. Balicas, et al., Nat. Mater. 9 (2010) 430.
[9] L. Song, L. Ci, H. Lu, P.B. Sorokin, C. Jin, J. Ni, A.G. Kvashnin, D.G. Kvashnin, J. Lou, B.I. Yakobson, Pulickel M. Ajayan, Nano Lett. 10 (2010) 3209.
[10] S. Azevedo, F. Moraes, B. Lima Bernardo, Appl. Phys. A 117 (2014) 2095.
[11] M.P. Levendorf, C.-J. Kim, L. Brown, P.Y. Huang, R.W. Havener, D.A. Muller, J. Park, Nature 488 (2012) 627.
[12] G.H. Han, J.A. Rodriguez-Manzo, C.-W. Lee, N.J. Kybert, M.B. Lerner, Z.J. Qi, E.N. Dattoli, A.M. Rappe, M. Drndic, A.T.C. Johnson, ACS Nano 7 (2013) 10129.
[13] L. Liu, J. Park, D.A. Siegel, K.F. McCarty, K.W. Clark, W. Deng, L. Basile, J.C. Idrobo, A.-P. Li, G. Gu, Science 343 (2014) 163.
[14] M. Liu, Y. Li, P. Chen, J. Sun, D. Ma, Q. Li, T. Gao, Y. Gao, Z. Cheng, X. Qiu, Y. Fang, Y. Zhang, Z. Liu, Nano Lett. 14 (2014) 6342.
[15] F. Bonaccorso, Z. Sun, T. Hasan, A.C. Ferrari, Nat. Photon. 4 (2010) 611.
[16] P. Avouris, F. Xia, MRS Bull. 37 (2012) 1225.
[17] K.S. Novoselov, V.I. Falko, L. Colombo, P.R. Gellert, M.G. Schwab, K. Kim, Nature 490 (2012) 192.
[18] F.H.L. Koppens, T. Mueller, P. Avouris, A.C. Ferrari, M.S. Vitiello, M. Polini, Nat. Nano 9 (2014) 780.
[19] G. Pirruccio, L.M. Moreno, G. Lozano, J.G. Rivas, ACS Nano 7 (2013) 4810.
[20] P. Avouris, F. Xia, MRS Bull. 37 (2012) 1225.
[21] D. Sanchez-Portal, P. Ordejon, E. Artacho, J.M. Soler, Int. J. Quantum Chem. 65 (1997) 453.
[22] W. Kohn, L.J. Sham, Phys. Rev. 140 (1965) A1133.
[23] J.P. Perdew, K. Burke, M. Ernzerhof, Phys. Rev. Lett. 77 (1996) 3865.
[24] N. Troullier, J.L. Martins, Phys. Rev. B 43 (1991) 1993.
[25] G.P.P. Giuseppe Grosso, Solid State Physics, 2nd ed., Academic Press, 2013.
[26] G.G. Martin Dressel, Electrodynamics of Solids: Optical Properties of Electrons in Matter, 1st ed., Cambridge University Press, 2002.
[27] S. Azevedo, Phys. Lett. A 351 (2006) 109.
[28] J.P. Guedes, S. Azevedo, M. Machado, Eur. Phys. J. B 80 (2011) 127.
[29] T. Cao, J. Feng, E.G. Wang, Phys. Rev. B 84 (2011) 205447.
[30] A. Ranjbar, M.S. Bahramy, M. Khazaei, H. Mizuseki, Y. Kawazoe, Phys. Rev. B 82 (2010) 165446.
[31] S. Casolo, O.M. Løvvik, R. Martinazzo, G.F. Tantardini, J. Chem. Phys. 130 (2009) 054704.
[32] E.J. Duplock, M. Scheffler, P.J.D. Lindan, Phys. Rev. Lett. 92 (2004) 225502.
[33] J. Singleton, Band Theory and Electronic Properties of Solids, Oxford University Press, Oxford, 2001.